J Math Chem (2012) 50:2202–2222
DOI 10.1007/s10910-012-0025-7

ORIGINAL PAPER

Importance of the proligand-promolecule model in stereochemistry. I. The unit-subduced-cycle-index (USCI) approach to geometric features of prismane derivatives

Shinsaku Fujita

Received: 11 April 2012 / Accepted: 18 April 2012 / Published online: 29 April 2012

Abstract Among the four methods of the unit-subduced-cycle-index (USCI) approach (Fujita in Symmetry and Combinatorial Enumeration in Chemistry. Springer, Berlin, Heidelberg, 1991), the fixed-point-matrix (FPM) method and the partial-cycle-index (PCI) method have been applied to the combinatorial enumeration of prismane derivatives. These enumeration processes are based on the proligand-promolecule model, which enables us to take account of achiral and chiral proligands. Prochirality in a geometric meaning has been discussed in general by emphasizing the presence of enantiospheric orbits in enumerated prismane derivatives. An enantiospheric orbit accommodating chiral proligands (along with achiral ones) has been shown to exhibit prochirality by using various prismane derivatives as examples. On the other hand, the scope of pseudoasymmetry has been extended to cover such a rigid skeleton as prismane in addition to a usual pseudoasymmetric center as a single atom, where the proligand-promolecule model plays an essential role.

Keywords Prismane · Enumeration · Stereochemistry · Proligand · Promolecule · Prochiral · Pseudoasymmetry

1 Introduction

1.1 Problem of the 2D–3D extension implied in stereochemistry

From its foundation by van't Hoff [1,2] and Le Bel [3] during the 1870s, stereochemistry has been based on the methodology in which two-dimensional (2D) structures

S. Fujita (✉)
Shonan Institute of Chemoinformatics and Mathematical Chemistry, Kaneko 479-7 Ooimachi, Ashigara-Kami-Gun, Kanagawa-Ken 258-0019, Japan
e-mail: shinsaku_fujita@nifty.com

(graphs) are extended into three-dimensional (3D) structures. The extension of 2D to 3D structures (the 2D–3D extension) has caused serious confusion in the progress of stereochemistry. For example, the original concept of "asymmetric tetrahedral carbon" proposed by van't Hoff was found to be insufficient in supporting the 2D–3D extension by Fischer's discovery of the stereoisomer number of trihydroglutaric acids [4–6]. This was tentatively rationalized by the concept of "pseudoasymmetric carbon centers" as exceptional cases of the original "asymmetric tetrahedral carbon".

The problem of the 2D–3D extension (e.g., asymmetry vs. pseudoasymmetry) revived during 1960s and 1970s, when the Cahn–Ingold–Prelog (CIP) system for assigning *RS*-descriptors were founded. Although the CIP system claimed "Specification of Molecular Chirality" as found in the title of the original proposal [7], the scope of the CIP system has covered "asymmetric" cases (chiral) and "pseudoasymmetric" cases (achiral). The problem of the CIP system has been avoided by the revision of its basis from chirality to stereogenicity [8], after the detailed investigation of pseudoasymmetry [9], as described concisely in the Nobel Prize lecture of Prelog (1975) [10]. Although the term "stereogenic" was separated from chirality, the separation was incomplete, so that the term "stereogenic units" turned out to connote a "chirality" plane, a "chirality" axis, "pseudoasymmetric" stereogenic units, etc. in an entangled fashion. Hence, we are safe to say that the problem of the 2D–3D extension has resulted in such transmutation of the term "chirality" as providing a misleading inclusion, i.e., chirality $\subset$ stereogenicity, although chirality and stereogenicity are independent concepts.

The confusion about "chirality" and "stereogenicity", which stemmed from the problem of the 2D–3D extension as described above, has also influenced the connotation of the term "prochiral" proposed as the basis of *pro-R/pro-S*-descriptors by Hanson [11]. The usage of "prochirality" with reference to prostereoisomerism was strongly suggested to be altogether abandoned by Mislow and Siegel [12] after emphasizing the importance of the local symmetry. However, the entangled situations for "prochirality" have not been settled even now in the conventional stereochemistry, as pointed out in the IUPAC Recommendations 1996 [13].

As for quantitative discussions, on the other hand, Pólya's theorem has been widely used as a method for counting graphs and chemical compounds [14,15]. However, Pólya's theorem itself was incapable of counting chemical compounds as 3D structures, so that it suffered from the problem of the 2D–3D extension, as pointed out in a review [16]. For example, Pólya's theorem was successful to count alkanes as graphs (or 2D structures), but Otter's dissimilarity characteristic equation for trees was necessary additionally in order to enumerate chiral and achiral alkanes as 3D structures [17]. For the purpose of settling the problem of the 2D–3D extension, a more general approach should be developed so as to improve Pólya's theorem.

1.2 Proligand-promolecule model for settling the problem of the 2D–3D extension

The problem of the 2D–3D extension has been detailedly investigated by Fujita, where the point-group theory and the permutation group theory are integrated to generate the concept of *subduction of coset representations* [18,19] and the relevant concept of *sphericities of orbits* [20–23]. These concepts have been applied to symmetry-itemized enumeration of 3D structures [24] and systematic classifications of organic compounds [25] in terms of the unit-subduced-cycle-index (USCI) approach [26].

The crux for settling the problem of the 2D–3D extension in the USCI approach is an explicit formulation of *the proligand-promolecule model* [27–29] where the sphericity of an orbit determines the mode of accommodating proligands [20–23]. As summarized in Chapter 21 of Fujita's book [26], the term *proligand* has been defined as a 3D object that is structureless but has chirality and the term *promolecule* has been defined as a 3D object that consists of a skeleton and such proligands. Such a skeleton for the proligand-promolecule model can be selected from any rigid skeletons, e.g., a tetrahedral skeleton [30], an ethane skeleton [28,31], an oxirane skeleton [32], an adamantane skeleton [27,30], a biphenyl skeleton [27], an allene skeleton [33,34], $\mathbf{D}_{3h}$-skeletons such as a trigonal bipyramid, an iceane skeleton, and prismane skeleton [35], $\mathbf{D}_{6h}$-skeletons such as a benzene skeleton and a coronene skeleton [36], a cyclohexane skeleton [37], a square planar skeleton [38], an octahedral skeleton [29], a dodecahedrane skeleton [39,40], a triptycene skeleton [41], a fullerene-C_{60} skeleton [42], and a cubane skeleton [43].

The above-mentioned shortage of Pólya's theorem has been overcome by Fujita's proligand method [44–46], where the concept of *sphericities of orbits* has been extended to the concept of *sphericities of cycles*, which means the adoption of the proligand-promolecule model for the purpose of settling the problem of the 2D–3D extension. Fujita's proligand method has been applied to the enumeration of alkanes and mono-substituted alkanes as 3D entities [47,48]. Fujita's proligand method and relevant methods have been applied for gross enumeration of cubane derivatives as 3D entities [49,50].

1.3 Aims of the present article

The main target of the present article is to discuss geometrical aspects of stereochemistry by using a prismane skeleton, which serves as a polycyclic skeleton for the proligand-promolecule model. After prismane derivatives are enumerated as 3D entities by the USCI approach based on the proligand-promolecule model, their chirality and prochirality are discussed in a purely geometric meaning. In particular, because the conventional terms "prochirality" and "pseudoasymmetry" have been influenced noticeably by the confusion due to the transmuted "chirality", they are reexamined from a purely geometric viewpoint of chirality.

2 Geometrical properties of prismane derivatives

2.1 Orbits and coset representations for the $\mathbf{D}_{3h}$-point group

According to the proligand-promolecule model (cf. Chapter 21 of Ref. [26]), a prismane skeleton **1** is regarded as a rigid skeleton which accommodates proligands to give promolecules. The six vertices (substitution sites) of the prismane skeleton **1** are

Fig. 1 Trigonal prismatic skeleton with reference numbering

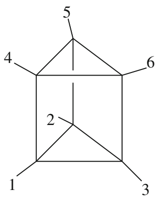

1

numbered sequentially as depicted in Fig. 1, where the mode of numbering is selected arbitrarily without losing generality.

The prismane skeleton **1** has a three-fold axis (elements: C_3 and C_3^2 as well as S_3 and S_3^5), three dihedral two-fold axes (elements: $C_{2(1)}, C_{2(2)}, C_{2(3)}$), three mirror planes containing the three-fold axis (elements: $\sigma_{v(1)}, \sigma_{v(2)}, \sigma_{v(3)}$), and a horizontal mirror plane containing the three dihedral two-fold axes (element: σ_h). Thus the global symmetry of **1** is characterized by the point group $\mathbf{D}_{3h}$ of order 12, which is composed of the following elements:

$$\mathbf{D}_{3h} = \{I, C_3, C_3^2, C_{2(1)}, C_{2(2)}, C_{2(3)}; \sigma_h, S_3, S_3^5, \sigma_{v(1)}, \sigma_{v(2)}, \sigma_{v(3)}\}, \tag{1}$$

among which the six elements before a semicolon are (proper) rotations, while the six elements after the semicolon are rotoreflections (improper rotations).

The point group $\mathbf{D}_{3h}$ of the skeleton **1** is characterized by the following non-redundant set of subgroups (SSG):

$$\mathrm{SSG}_{\mathbf{D}_{3h}} = \{\mathbf{C}_1, \mathbf{C}_2, \mathbf{C}_s, \mathbf{C}'_s, \mathbf{C}_3, \mathbf{C}_{2v}, \mathbf{C}_{3v}, \mathbf{C}_{3h}, \mathbf{D}_3, \mathbf{D}_{3h}\}, \tag{2}$$

where each subgroup is selected as a representative of relevant conjugate subgroups and where these subgroups are aligned in an ascending order of their orders. For example, the subgroup $\mathbf{C}_s$ (order: $|\mathbf{C}_s| = 2$) listed in Eq. (2) is a representative selected from conjugate subgroups, i.e., $\{I, C_{2(1)}\}$ $(= \mathbf{C}_s)$, $\{I, C_{2(2)}\}$, and $\{I, C_{2(3)}\}$.

The six vertices (substitution sites) of the prismane skeleton **1** are equivalent under the action of $\mathbf{D}_{3h}$ so as to construct an orbit (an equivalence class). According to the USCI approach [26], the orbit is governed by the coset representation $\mathbf{D}_{3h}(/\mathbf{C}_s)$, where the subgroup $\mathbf{C}_s$ $(= \{I, C_{2(1)}\})$ represents the local symmetry of each vertex of **1**.

The coset representation $\mathbf{D}_{3h}(/\mathbf{C}_s)$ is calculated algebraically on the basis of a coset decomposition of $\mathbf{D}_{3h}$ by $\mathbf{C}_s$, which gives the following set of permutations represented as products of cycles [25]:

$$\left.\begin{array}{rcc} I & \sim & (1)(2)(3)(4)(5)(6) \\ C_3 & \sim & (1\ 2\ 3)(4\ 5\ 6) \\ C_3^2 & \sim & (1\ 3\ 2)(4\ 6\ 5) \\ C_{2(1)} & \sim & (1\ 4)(2\ 6)(3\ 5) \\ C_{2(2)} & \sim & (1\ 6)(2\ 5)(3\ 4) \\ C_{2(3)} & \sim & (1\ 5)(2\ 4)(3\ 6) \end{array}\right\} \text{(proper) rotations} \tag{3}$$

$$\left.\begin{array}{lcl} \sigma_h & \sim & \overline{(1\ 4)(2\ 5)(3\ 6)} \\ S_3 & \sim & \overline{(1\ 5\ 3\ 4\ 2\ 6)} \\ S_3^5 & \sim & \overline{(1\ 6\ 2\ 4\ 3\ 5)} \\ \sigma_{v(1)} & \sim & \overline{(1)(2\ 3)(4)(5\ 6)} \\ \sigma_{v(2)} & \sim & \overline{(1\ 3)(2)(4\ 6)(5)} \\ \sigma_{v(3)} & \sim & \overline{(1\ 2)(3)(4\ 5)(6)} \end{array}\right\} \text{rotoreflections (improper rotations)} \tag{4}$$

where each product of cycles with an overline is concerned with a rotoreflection. Such an explicit notation as an overline claims the alternation of chirality senses of proligands at issue [38]. The degree of the coset representation $\mathbf{D}_{3h}(/\mathbf{C}_s)$ is calculated to be 6 (i.e., $|\mathbf{D}_{3h}|/|\mathbf{C}_s| = 12/2 = 6$), which is equal to the number of vertices contained in the prismane skeleton **1**. A full set of coset representations for $\mathbf{D}_{3h}$ has been reported in Ref. [25]. Prismane itself has been characterized by the set-of-coset-representation (SCR) notation, i.e., $\mathbf{D}_{3h}[2/\mathbf{C}_s(\mathrm{C}_6, \mathrm{H}_6)]$, which means that the six carbon atoms belong to a $\mathbf{D}_{3h}(/\mathbf{C}_s)$-orbit and the six hydrogen atoms belong also to another $\mathbf{D}_{3h}(/\mathbf{C}_s)$-orbit [25]. If only substituents are taken into consideration, we use a simplified SCR notation, $\mathbf{D}_{3h}[/\mathbf{C}_s(\mathrm{H}_6)]$.

2.2 Subduction of coset representations

According to the USCI approach [26,51], a promolecule derived from a skeleton has a set of suborbits which are generated by the subdivisions of an original orbit. The process of the subdivision is controlled by the subduction of a coset representation. For example, a $\mathbf{C}_s$-molecule is generated by fixing the corresponding mirror plane containing the vertices 1 and 4, when an achiral proligand A is placed on the vertex 1 and five hydrogen atoms are placed on the remaining vertices to give a derivative **2** of the constitution of substituents, $\mathrm{H}_5\mathrm{A}$. This process of derivation is controlled by the following subduction of the coset representation $\mathbf{D}_{3h}(/\mathbf{C}_s)$ into the subgroup $\mathbf{C}_s$, i.e.,

$$\mathbf{D}_{3h}(/\mathbf{C}_s) \downarrow \mathbf{C}_s = \underbrace{2\mathbf{C}_s(/\mathbf{C}_1)}_{\{2,3\},\,\{5,6\}} + \underbrace{2\mathbf{C}_s(/\mathbf{C}_s)}_{\{1\},\,\{4\}}. \tag{5}$$

Note that the five hydrogen atoms are distributed into a one-membered $\mathbf{C}_s(/\mathbf{C}_s)$-orbit (orbit size: $|\mathbf{C}_s|/|\mathbf{C}_s| = 1/1 = 1$) and two-membered $\mathbf{C}_s(/\mathbf{C}_1)$-orbits (orbit size: $|\mathbf{C}_s|/|\mathbf{C}_1| = 2/1 = 2$). According to this subduction, promolecules **3** ($\mathrm{H}_3\mathrm{A}_3$) and **4** ($\mathrm{H}_3\mathrm{A}\mathrm{p}\overline{\mathrm{p}}$) having $\mathbf{C}_s$-symmetry can be derived in a similar way to **2**, where the letter A represents an achiral proligand and the letters p and $\overline{\mathrm{p}}$ represent a pair of enantiomeric proligands in isolation.

The resulting promolecules (Fig. 2) are characterized by the following SCR notations:

$$\mathbf{C}_s[2/\mathbf{C}_1(2\mathrm{H}_2); 2/\mathbf{C}_s(\mathrm{A}, \mathrm{H})] \text{ for } \mathbf{2} \tag{6}$$
$$\mathbf{C}_s[2/\mathbf{C}_1(\mathrm{A}_2, \mathrm{H}_2); 2/\mathbf{C}_s(\mathrm{A}, \mathrm{H})] \text{ for } \mathbf{3} \tag{7}$$
$$\mathbf{C}_s[2/\mathbf{C}_1(\mathrm{H}_2, \mathrm{p}\overline{\mathrm{p}}); 2/\mathbf{C}_s(\mathrm{A}, \mathrm{H})] \text{ for } \mathbf{4} \tag{8}$$

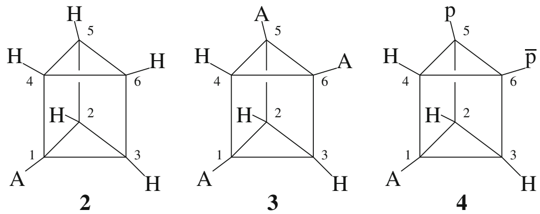

Fig. 2 Examples of prismane derivatives of $\mathbf{C}_s$-symmetry. The symbol *A* represents an achiral proligand in isolation. A pair of *p* and $\bar{p}$ represents a pair of enantiomeric proligands in isolation

where carbon atoms are omitted for simplicity's sake. The subduction data for a $\mathbf{D}_{3h}$-group have been calculated algebraically [25] and summarized in Table 12 of Ref. [25] and in Appendix C of [26].

2.3 Sphericities of orbits and chirality fittingness

According to the USCI approach [20,26,51], an orbit belonging to a coset representation $\mathbf{G}(/\mathbf{G}_i)$ is categorized into a homospheric ($\mathbf{G}$ and $\mathbf{G}_i$: achiral), enantiospheric ($\mathbf{G}$: achiral; and $\mathbf{G}_i$: chiral), or hemispheric orbit ($\mathbf{G}$ and $\mathbf{G}_i$: chiral). The sphericity controls the mode of accommodation of the orbit, which is called *chirality fittingness* [20,26]. The chirality fittingness shows that a homospheric orbit accommodates a set of achiral proligands of the same kind, and a hemispheric orbit accommodates a set of chiral or achiral proligands of the same kind. An enantiospheric orbit exhibits a special mode of chirality fittingness, because it is subdivided into two halves as a result of the local chirality of the orbit at issue. If achiral proligands are taken into consideration, the two halves of an enantiospheric orbit can accommodate a set of achiral proligands of the same kind. If chiral proligands are taken into consideration, one half accommodates a set of chiral proligands of a given chirality sense and the other half accommodates a set of chiral proligands with an opposite chirality sense. The latter mode of accommodation for chiral promolecules is found in the promolecule **4**, where one of the $\mathbf{C}_s(/\mathbf{C}_1)$-orbits accommodates two hydrogens (as achiral proligands) and the other accommodates a pair of p and $\overline{\mathrm{p}}$ (as chiral proligands).

The two halves of an enantiospheric orbit are in an enantiotopic relationship, which is extended to refer to such two halves, each having one or more substitution sites. Note that the original connotation of term *enantiotopic* refers to a relationship between two substitution sites. Although we are able to discuss geometric features of stereochemistry by using such attributive terms as sphericities or by using such relational terms as topicities, the former attributive terms are more decisive because they are based on the concept of orbits.

3 Enumeration by the fixed-point-matrix (FPM) method

The USCI approach supports four methods of symmetry-itemized enumeration [26]. This section is devoted to the enumeration of prismane derivatives by means of the fixed-point-matrix (FPM) method as one of the four methods of the USCI approach. The FPM method is capable of treating any rigid skeletons (e.g., a prismane skeleton) because of the underlying proligand-promolecule model. Gross enumeration of prismane derivatives (without symmetry-itemization) has been reported by applying Fujita's proligand method [52].

3.1 Sphericity indices and USCI-CFs

Let us assign a sphericity index a_d, c_d, or b_d to an orbit according to its sphericity, where a sphericity index a_d is assigned to a d-membered homospheric orbit, a sphericity index c_d to a d-membered enantiospheric orbit, and a sphericity index b_d to a d-membered hemispheric orbit. Thereby, the subduction of a coset representation is characterized by a product of such sphericity indices, which is called a unit subduced cycle index with chirality fittingness (USCI-CF). For example, the subduction represented by Eq. (5) is characterized by the corresponding USCI-CF, i.e., $a_1^2 c_2^2$. The complete list of such USCI-CFs (along with USCIs) for the point group $\mathbf{D}_{3h}$ has been calculated algebraically [25,35] and collected in a tabular form (a USCI-CF table) in Appendix E of a book [26].

For the purpose of enumerating prismane derivatives, the $\mathbf{D}_{3h}(/\mathbf{C}_s)$-row of such a USCI-CF table (e.g., Table E.13 of Ref. [26]) is necessary. Thereby we obtain a formal row vector as follows:

$$\text{USCI-CF}_{\mathbf{D}_{3h}(/\mathbf{C}_s)} = (b_1^6, b_2^3, a_1^2 c_2^2, c_2^3, b_3^2, a_2 c_4, a_3^2, c_6, b_6, a_6), \tag{9}$$

where the USCI-CFs are aligned according to the order of the SSG (Eq. 2).

3.2 Enumeration of prismane derivatives by the FPM method

Suppose that proligands for vertex substitution are selected from the following proligand inventory:

$$\mathbf{L} = \{\mathrm{H}, \mathrm{A}, \mathrm{W}, \mathrm{X}, \mathrm{Y}, \mathrm{Z}, \mathrm{p}, \overline{\mathrm{p}}, \mathrm{q}, \overline{\mathrm{q}}\}, \tag{10}$$

where the letters H, A, W, X, Y, and Z denote achiral proligands and a pair of p/$\overline{\mathrm{p}}$ or q/$\overline{\mathrm{q}}$ denotes a pair of enantiomeric proligands in isolation (when detached).

Because we take only one orbit of the six substitution sites of **1** into consideration, the USCI-CF vector of Eq. (9) (the $\mathbf{D}_{3h}(/\mathbf{C}_s)$-row of the USCI-CF table) can be regarded as the corresponding list of subduced cycle indices with chirality fittingness (SCI-CFs). According to the FPM method [26], each SCI-CF (or USCI-CF in this case) is capable of evaluating the number of fixed points on the action of the relevant subgroup, where respective sphericity indices contained in the SCI-CF are substituted by the following inventory functions:

$$a_d = \mathrm{H}^d + \mathrm{A}^d + \mathrm{W}^d + \mathrm{X}^d + \mathrm{Y}^d + \mathrm{Z}^d \tag{11}$$

$$b_d = \mathrm{H}^d + \mathrm{A}^d + \mathrm{W}^d + \mathrm{X}^d + \mathrm{Y}^d + \mathrm{Z}^d + \mathrm{p}^d + \overline{\mathrm{p}}^d + \mathrm{q}^d + \overline{\mathrm{q}}^d \tag{12}$$

$$c_d = \mathrm{H}^d + \mathrm{A}^d + \mathrm{W}^d + \mathrm{X}^d + \mathrm{Y}^d + \mathrm{Z}^d + 2\mathrm{p}^{d/2}\overline{\mathrm{p}}^{d/2} + 2\mathrm{p}^{d/2}\overline{\mathrm{p}}^{d/2}. \tag{13}$$

The power $d/2$ appearing in Eq. (13) is an integer because the subscript d of the sphericity index c_d is always even in the light of the enantiosphericity of the corresponding orbit [26].

These inventory functions for vertices (Eqs. 11–13) are introduced into an SCI-CF to give a generating function, in which the coefficient of the term:

$$\mathrm{H}^{n_\mathrm{H}}\mathrm{A}^{n_\mathrm{A}}\mathrm{W}^{n_\mathrm{W}}\mathrm{X}^{n_\mathrm{X}}\mathrm{Y}^{n_\mathrm{Y}}\mathrm{Z}^{n_\mathrm{Z}}\mathrm{p}^{n_\mathrm{p}}\overline{\mathrm{p}}^{n_{\overline{\mathrm{p}}}}\mathrm{q}^{n_\mathrm{q}}\overline{\mathrm{q}}^{n_{\overline{\mathrm{q}}}} \tag{14}$$

indicates the number of fixed promolecules to be counted, where the powers are non-negative integers which satisfy the following relationship:

$$n_\mathrm{H} + n_\mathrm{A} + n_\mathrm{W} + n_\mathrm{X} + n_\mathrm{Y} + n_\mathrm{Z} + n_\mathrm{p} + n_{\overline{\mathrm{p}}} + n_\mathrm{q} + n_{\overline{\mathrm{q}}} = 6 \tag{15}$$

The term shown in Eq. (14) can be represented by the following partition:

$$[\theta] = [n_\mathrm{H}, n_\mathrm{A}, n_\mathrm{W}, n_\mathrm{X}, n_\mathrm{Y}, n_\mathrm{Z}; n_\mathrm{p}, n_{\overline{\mathrm{p}}}, n_\mathrm{q}, n_{\overline{\mathrm{q}}}], \tag{16}$$

where we can presume $n_\mathrm{H} \geq n_\mathrm{A} \geq n_\mathrm{W} \geq n_\mathrm{X} \geq n_\mathrm{Y} \geq n_\mathrm{Z} \geq 0$; $n_\mathrm{p} \geq n_{\overline{\mathrm{p}}} \geq 0$; and $n_\mathrm{q} \geq n_{\overline{\mathrm{q}}} \geq 0$ without losing generality.

For example, the SCI-CF $a_1^2 c_2^2$ for the subgroup $\mathbf{C}_s$ (Eq. 9) generates the following generating function by introducing the inventory functions (Eqs. 11–13):

$$\begin{aligned} g_{\mathbf{C}_s} = {} & \mathrm{H}^6 + 2(\mathrm{H}^5\mathrm{A} + \cdots) + 3(\mathrm{H}^4\mathrm{A}^2 + \cdots) \\ & + 2(\mathrm{H}^4\mathrm{AW} + \cdots) + 4\mathrm{H}^4\mathrm{p}\overline{\mathrm{p}} + \cdots + \end{aligned} \tag{17}$$

Thereby, the coefficient 3 of the term $3(\mathrm{H}^4\mathrm{A}^2 + \cdots)$ in the right-hand side of Eq. (17) indicates the number ($\rho_{[\theta]_1\mathbf{C}_s}$) of fixed promolecules of the term $\mathrm{H}^4\mathrm{A}^2$ (and $\mathrm{H}^4\mathrm{W}^2$ etc.) or the partition $[\theta]_1 = [4, 2, 0, 0, 0, 0; 0, 0, 0, 0]$ under the action of the subgroup $\mathbf{C}_s$, i.e.,

$$\rho_{[\theta]_1\mathbf{C}_s} = 3. \tag{18}$$

This process for obtaining $\rho_{[\theta]_1\mathbf{C}_s}$ is repeated to cover all of the SCI-CFs collected in Eq. (9) (corresponding to the subgroups collected in Eq. 2) so as to give the numbers of fixed points, i.e., $\rho_{[\theta]_1\mathbf{G}_j}$ ($\mathbf{G}_j \in \mathrm{SSG}_{\mathbf{D}_{3h}}$), which are collected to form a fixed-point vector (FPV) as follows:

$$\mathrm{FPV}_1 = (\rho_{[\theta]_1\mathbf{C}_1}, \rho_{[\theta]_1\mathbf{C}_2}, \rho_{[\theta]_1\mathbf{C}_s}, \ldots, \rho_{[\theta]_1\mathbf{D}_{3h}}) = (15, 3, 3, 3, 0, 1, 0, 0, 0, 0). \tag{19}$$

Note that the elements in Eq. (19) are aligned in accord with the appearance order of Eq. (2). In a similar way, the FPVs for several partitions:

$$[\theta]_1 = [4, 2, 0, 0, 0, 0; 0, 0, 0, 0] \quad \text{for } \mathrm{H}^4\mathrm{A}^2 \tag{20}$$
$$[\theta]_2 = [4, 0, 0, 0, 0, 0; 2, 0, 0, 0] \quad \text{for } \mathrm{H}^4\mathrm{p}^2 \tag{21}$$
$$[\theta]_3 = [4, 1, 1, 0, 0, 0; 0, 0, 0, 0] \quad \text{for } \mathrm{H}^4\mathrm{AW} \tag{22}$$

$$[\theta]_4 = [4, 1, 0, 0, 0, 0; 1, 0, 0, 0] \quad \text{for } \mathrm{H}^4\mathrm{Ap} \tag{23}$$
$$[\theta]_5 = [4, 0, 0, 0, 0, 0; 1, 1, 0, 0] \quad \text{for } \mathrm{H}^4\mathrm{p}\overline{\mathrm{p}} \tag{24}$$
$$[\theta]_6 = [4, 0, 0, 0, 0, 0; 1, 0, 1, 0] \quad \text{for } \mathrm{H}^4\mathrm{pq} \tag{25}$$

are calculated and collected in a matrix form (named a fixed-point matrix (FPM)) as follows:

$$\mathrm{FPM}_1 = \begin{array}{c} [\theta]_1 \\ [\theta]_2 \\ [\theta]_3 \\ [\theta]_4 \\ [\theta]_5 \\ [\theta]_6 \end{array} \begin{pmatrix} 15 & 3 & 3 & 3 & 0 & 1 & 0 & 0 & 0 & 0 \\ 15 & 3 & 0 & 0 & 0 & 0 & 0 & 0 & 0 & 0 \\ 30 & 0 & 2 & 0 & 0 & 0 & 0 & 0 & 0 & 0 \\ 30 & 0 & 0 & 0 & 0 & 0 & 0 & 0 & 0 & 0 \\ 30 & 0 & 4 & 6 & 0 & 0 & 0 & 0 & 0 & 0 \\ 30 & 0 & 0 & 0 & 0 & 0 & 0 & 0 & 0 & 0 \end{pmatrix}, \tag{26}$$

where each row represents the FPV$_i$ for the partition $[\theta]_i$ ($i = 1$ to 6), e.g., the first row corresponds to Eq. (19). The mark table for $\mathbf{D}_{3h}$ and the inverse mark table have been calculated algebraically [25,35] and collected in Table 6 of [25] and in Appendix B of a book [26]. The inverse mark table is shown as follows as a matrix form:

$$M^{-1}_{\mathbf{D}_{3h}} = \frac{1}{12} \begin{pmatrix} 1 & 0 & 0 & 0 & 0 & 0 & 0 & 0 & 0 & 0 \\ -3 & 6 & 0 & 0 & 0 & 0 & 0 & 0 & 0 & 0 \\ -3 & 0 & 6 & 0 & 0 & 0 & 0 & 0 & 0 & 0 \\ -1 & 0 & 0 & 2 & 0 & 0 & 0 & 0 & 0 & 0 \\ -1 & 0 & 0 & 0 & 3 & 0 & 0 & 0 & 0 & 0 \\ 6 & -6 & -6 & -6 & 0 & 12 & 0 & 0 & 0 & 0 \\ 3 & 0 & -6 & 0 & -3 & 0 & 6 & 0 & 0 & 0 \\ 1 & 0 & 0 & -2 & -3 & 0 & 0 & 6 & 0 & 0 \\ 3 & -6 & 0 & 0 & -3 & 0 & 0 & 0 & 6 & 0 \\ -6 & 6 & 6 & 6 & 6 & -12 & -6 & -6 & -6 & 12 \end{pmatrix} \tag{27}$$

According to the FPM method of the USCI approach, the multiplication of the FPM (Eq. 26) by the inverse (Eq. 27) gives the following isomer-counting matrix (ICM):

$$\mathrm{ICM}_1 = \mathrm{FPM}_1 \times M^{-1}_{\mathbf{D}_{3h}} = \begin{array}{c} [\theta]_1 \\ [\theta]_2 \\ [\theta]_3 \\ [\theta]_4 \\ [\theta]_5 \\ [\theta]_6 \end{array} \begin{pmatrix} 0 & 1 & 1 & 0 & 0 & 1 & 0 & 0 & 0 & 0 \\ \frac{1}{2} & \frac{3}{2} & 0 & 0 & 0 & 0 & 0 & 0 & 0 & 0 \\ 2 & 0 & 1 & 0 & 0 & 0 & 0 & 0 & 0 & 0 \\ \frac{5}{2} & 0 & 0 & 0 & 0 & 0 & 0 & 0 & 0 & 0 \\ 1 & 0 & 2 & 1 & 0 & 0 & 0 & 0 & 0 & 0 \\ \frac{5}{2} & 0 & 0 & 0 & 0 & 0 & 0 & 0 & 0 & 0 \end{pmatrix} \tag{28}$$

The value at the intersection between the $[\theta]_i$-row ($i = 1$ to 6) and the $\mathbf{G}_j$th column ($\mathbf{G}_j \in \mathrm{SSG}_{\mathbf{D}_{3h}}$) represents the number of isomers with the constitution $[\theta]_i$ and $\mathbf{G}_j$-symmetry. It should be noted that the value $\frac{1}{2}$ or $\frac{3}{2}$ in the $[\theta]_2$-row of the matrix of Eq. (28) should be interpreted to be $1 \times \frac{1}{2}(\mathrm{H}^4\mathrm{p}^2 + \mathrm{H}^4\overline{\mathrm{p}}^2)$ or $3 \times \frac{1}{2}(\mathrm{H}^4\mathrm{p}^2 + \mathrm{H}^4\overline{\mathrm{p}}^2)$, which indicates the presence of one or three pairs of enantiomers $\mathrm{H}^4\mathrm{p}^2$ and $\mathrm{H}^4\overline{\mathrm{p}}^2$, because the term $\frac{1}{2}(\mathrm{H}^4\mathrm{p}^2 + \mathrm{H}^4\overline{\mathrm{p}}^2)$ corresponds to such a pair of enantiomers.

4 Enumeration by the partial-cycle-index (PCI) method

This section is devoted to the enumeration of prismane derivatives by means of the partial-cycle-index (PCI) method as one of the four methods of the USCI approach [26]. The PCI method is capable of treating any rigid skeletons (e.g., a prismane skeleton) because of the underlying proligand-promolecule model.

4.1 Enumeration of prismane derivatives by the PCI method

In order to solve the same problem of enumeration as described above, the PCI method of the USCI approach calculates partial cycle indices with chirality fittingness (PCI-CFs), where the alignment of SCI-CFs shown in Eq. (9) (USCI-CF$_{\mathbf{D}_{3h}(/\mathbf{C}_s)}$) is regarded as a formal vector and multiplied by the inverse matrix (Eq. 27). Thereby, the following formal calculation is possible:

$$\text{USCI-CF}_{\mathbf{D}_{3h}(/\mathbf{C}_s)} \times M^{-1}_{\mathbf{D}_{3h}} = (\text{PCI}_{\mathbf{C}_1}, \text{PCI}_{\mathbf{C}_2}, \ldots, \text{PCI}_{\mathbf{D}_{3h}}). \tag{29}$$

Each element of the resulting formal vector represents a PCI-CF for each subgroup of $\mathbf{D}_{3h}$ as follows:

$$\begin{aligned}
\text{PCI}_{\mathbf{C}_1} &= \frac{1}{12}b_1^6 - \frac{1}{4}b_2^3 - \frac{1}{4}a_1^2c_2^2 - \frac{1}{12}c_2^3 - \frac{1}{12}b_3^2 \\
&\quad + \frac{1}{2}a_2c_4 + \frac{1}{4}a_3^2 + \frac{1}{12}c_6 + \frac{1}{4}b_6 - \frac{1}{2}a_6 &(30)\\
\text{PCI}_{\mathbf{C}_2} &= \frac{1}{2}b_2^3 - \frac{1}{2}a_2c_4 - \frac{1}{2}b_6 + \frac{1}{2}a_6 &(31)\\
\text{PCI}_{\mathbf{C}_s} &= \frac{1}{2}a_1^2c_2^2 - \frac{1}{2}a_2c_4 - \frac{1}{2}a_3^2 + \frac{1}{2}a_6 &(32)\\
\text{PCI}_{\mathbf{C}'_s} &= \frac{1}{6}c_2^3 - \frac{1}{2}a_2c_4 - \frac{1}{6}c_6 + \frac{1}{2}a_6 &(33)\\
\text{PCI}_{\mathbf{C}_3} &= \frac{1}{4}b_3^2 - \frac{1}{4}a_3^2 - \frac{1}{4}c_6 - \frac{1}{4}b_6 + \frac{1}{2}a_6 &(34)\\
\text{PCI}_{\mathbf{C}_{2v}} &= a_2c_4 - a_6 &(35)\\
\text{PCI}_{\mathbf{C}_{3v}} &= \frac{1}{2}a_3^2 - \frac{1}{2}a_6 &(36)\\
\text{PCI}_{\mathbf{C}_{3h}} &= \frac{1}{2}c_6 - \frac{1}{2}a_6 &(37)\\
\text{PCI}_{\mathbf{D}_3} &= \frac{1}{2}b_6 - \frac{1}{2}a_6 &(38)\\
\text{PCI}_{\mathbf{D}_{3h}} &= a_6 &(39)
\end{aligned}$$

The inventory functions for vertex substitution (Eqs. 11–13) are introduced into the PCI-CFs (Eqs. 30–39). The resulting equations are expanded to give generating functions of respective subsymmetries (cf. SSG$_{\mathbf{D}_{3h}}$ of Eq. 2) for counting derivatives in a symmetry-itemized fashion, where the coefficient of the term (Eq. 14) gives the number of prismane derivatives as 3D objects. The coefficients of terms appearing in generating functions for respective subgroups are summarized in Table 1, where the rows are concerned with the terms (Eq. 14), which are represented by partitions (Eq. 16), while the columns are concerned with respective subgroups. Values in the row of a partition with an asterisk (*) should be duplicated, because the partition with (*), e.g., [5,0,0,0,0,0;1,0,0,0]* for the constitution H_5p, is accompanied with the partition of the corresponding enantiomer, e.g., [5,0,0,0,0,0;0,1,0,0]* for the constitution $H_5\overline{p}$, although the latter is omitted. Note that a pair of enantiomers are counted once. Thus the value 1/2 at the intersection between the [5,0,0,0,0,0;1,0,0,0]*-row and $\mathbf{C}_1$-column in Table 1 should be duplicated to give the number 1 in accord with the interpretation represented by the formula: $1 \times \frac{1}{2}(H^5p + H^5\overline{p})$.

5 Discussions

5.1 Geometric prochirality

The FPM method (the $[\theta]_1$-row of Eq. 28) and the PCI method (the [4, 2, 0, 0, 0, 0; 0, 0, 0, 0]-row of Table 1) indicates the presence of one pair of enantiomeric $\mathbf{C}_2$-promolecules, one $\mathbf{C}_s$-promolecule, and one $\mathbf{C}_{2v}$-promolecule for prismanes with the constitution H_4A_2. They are depicted in Fig. 3.

According to the USCI approach [26], prochirality in a geometric meaning (*geometric prochirality*) is linked with the presence of a least one enantiospheric orbit, as stated in Ref. [20]:

> An enantiospheric orbit is capable of separating into two hemispheric orbits of the same length under a chiral environment, whether the change is reversible or irreversible. A prochiral compound is defined as an achiral compound has at least one enantiospheric orbit.

This definition of *prochirality* is based on the sphericities of orbits, which are determined in a purely geometric fashion, so that the prochirality at issue is referred to as *geometric prochirality*. According to the membership criterion for topicity proposed in Ref. [20], the two halves producing the two hemispheric orbits are determined to be enantiotopic to each other in an achiral compound. A more comprehensive discussion on prochirality [53] and reviews on stereochemical features of prochirality [22,23] have appeared on the basis of the concept of sphericities.

The $\mathbf{C}_s$-promolecule **6** is generated in accord with the subduction represented by Eq. 5 or with the corresponding USCI-CF $a_1^2c_2^2$ (Eq. 9). Two achiral proligands A's occupy the two-membered enantiospheric $\mathbf{C}_s(/\mathbf{C}_1)$-orbit, i.e., {5, 6}, two hydrogens (as achiral proligands) occupy the other two-membered enantiospheric $\mathbf{C}_s(/\mathbf{C}_1)$-orbit, i.e., {2, 3}, and the remaining hydrogens separately occupy two one-membered homospheric $\mathbf{C}_s(/\mathbf{C}_s)$-orbits, i.e., {1} and {4}, one by one. The presence of two enantiospheric orbits indicates that the $\mathbf{C}_s$-promolecule **6** is prochiral in a geometric meaning. The two proligands A's (or the two hydrogens) of the enantiospheric orbit are differentiated under a chiral condition so as to generate promolecules of enantiomeric relationships.

Table 1 Numbers of prismane derivatives

	$\mathbf{C}_1$	$\mathbf{C}_2$	$\mathbf{C}_s$	$\mathbf{C}'_s$	$\mathbf{C}_3$	$\mathbf{C}_{2v}$	$\mathbf{C}_{3v}$	$\mathbf{C}_{3h}$	$\mathbf{D}_3$	$\mathbf{D}_{3h}$
[6,0,0,0,0,0;0,0,0,0]	0	0	0	0	0	0	0	0	0	1
[5,1,0,0,0,0;0,0,0,0]	0	0	1	0	0	0	0	0	0	0
[5,0,0,0,0,0;1,0,0,0]*	1/2	0	0	0	0	0	0	0	0	0
[4,2,0,0,0,0;0,0,0,0]	0	1	1	0	0	1	0	0	0	0
[4,0,0,0,0,0;2,0,0,0]*	1/2	3/2	0	0	0	0	0	0	0	0
[4,1,1,0,0,0;0,0,0,0]	2	0	1	0	0	0	0	0	0	0
[4,1,0,0,0,0;1,0,0,0]*	5/2	0	0	0	0	0	0	0	0	0
[4,0,0,0,0,0;1,1,0,0]	1	0	2	1	0	0	0	0	0	0
[4,0,0,0,0,0;1,0,1,0]*	5/2	0	0	0	0	0	0	0	0	0
[3,3,0,0,0,0;0,0,0,0]	1	0	1	0	0	0	1	0	0	0
[3,0,0,0,0,0;3,0,0,0]*	3/2	0	0	0	1/2	0	0	0	0	0
[3,2,1,0,0,0;0,0,0,0]	4	0	2	0	0	0	0	0	0	0
[3,2,0,0,0,0;1,0,0,0]*	5	0	0	0	0	0	0	0	0	0
[3,1,0,0,0,0;2,0,0,0]*	5	0	0	0	0	0	0	0	0	0
[3,0,0,0,0,0;2,1,0,0]*	5	0	0	0	0	0	0	0	0	0
[3,1,1,1,0,0;0,0,0,0]	10	0	0	0	0	0	0	0	0	0
[3,1,1,0,0,0;1,0,0,0]*	10	0	0	0	0	0	0	0	0	0
[3,1,0,0,0,0;1,1,0,0]	8	0	4	0	0	0	0	0	0	0
[3,1,0,0,0,0;1,0,1,0]*	10	0	0	0	0	0	0	0	0	0
[3,0,0,0,0,0;1,1,1,0]*	10	0	0	0	0	0	0	0	0	0
[2,2,1,1,0,0;0,0,0,0]	14	0	2	0	0	0	0	0	0	0
[2,2,1,0,0,0;1,0,0,0]*	15	0	0	0	0	0	0	0	0	0
[2,2,0,0,0,0;1,1,0,0]	12	0	4	2	0	0	0	0	0	0
[2,2,0,0,0,0;1,0,1,0]*	15	0	0	0	0	0	0	0	0	0
[2,1,1,0,0,0;2,0,0,0]*	15	0	0	0	0	0	0	0	0	0
[2,1,0,0,0,0;2,1,0,0]*	15	0	0	0	0	0	0	0	0	0
[2,1,0,0,0,0;2,0,1,0]*	15	0	0	0	0	0	0	0	0	0
[2,0,0,0,0,0;2,1,1,0]*	15	0	0	0	0	0	0	0	0	0
[2,1,1,1,1,0;0,0,0,0]	30	0	0	0	0	0	0	0	0	0
[2,1,1,1,0,0;1,0,0,0]*	30	0	0	0	0	0	0	0	0	0
[2,1,1,0,0,0;1,1,0,0]	28	0	4	0	0	0	0	0	0	0
[2,1,0,0,0,0;1,1,1,0]*	30	0	0	0	0	0	0	0	0	0
[2,0,0,0,0,0;1,1,1,1]	26	0	4	4	0	0	0	0	0	0
[1,1,1,1,1,1;0,0,0,0]	60	0	0	0	0	0	0	0	0	0
[1,1,1,1,0,0;1,0,1,0]*	60	0	0	0	0	0	0	0	0	0
[1,1,1,0,0,0;1,1,1,0]*	60	0	0	0	0	0	0	0	0	0
[1,1,0,0,0,0;1,1,1,1]	56	0	8	0	0	0	0	0	0	0
[0,0,0,0,0,0;6,0,0,0]*	0	0	0	0	0	0	0	0	1/2	0
[0,0,0,0,0,0;5,1,0,0]*	1/2	0	0	0	0	0	0	0	0	0
[0,0,0,0,0,0;5,0,1,0]*	1/2	0	0	0	0	0	0	0	0	0

Table 1 continued

	$\mathbf{C}_1$	$\mathbf{C}_2$	$\mathbf{C}_s$	$\mathbf{C}'_s$	$\mathbf{C}_3$	$\mathbf{C}_{2v}$	$\mathbf{C}_{3v}$	$\mathbf{C}_{3h}$	$\mathbf{D}_3$	$\mathbf{D}_{3h}$
[1,0,0,0,0,0;5,0,0,0]*	1/2	0	0	0	0	0	0	0	0	0
[0,0,0,0,0,0;4,2,0,0]*	1/2	3/2	0	0	0	0	0	0	0	0
[0,0,0,0,0,0;4,0,2,0]*	1/2	3/2	0	0	0	0	0	0	0	0
[2,0,0,0,0,0;4,0,0,0]*	1/2	3/2	0	0	0	0	0	0	0	0
[0,0,0,0,0,0;4,1,1,0]*	5/2	0	0	0	0	0	0	0	0	0
[1,0,0,0,0,0;4,1,0,0]*	5/2	0	0	0	0	0	0	0	0	0
[1,0,0,0,0,0;4,0,1,0]*	5/2	0	0	0	0	0	0	0	0	0
[1,1,0,0,0,0;4,0,0,0]*	5/2	0	0	0	0	0	0	0	0	0
[0,0,0,0,0,0;3,3,0,0]	1	0	0	1	0	0	0	1	0	0
[0,0,0,0,0,0;3,0,3,0]*	3/2	0	0	0	1/2	0	0	0	0	0
[3,0,0,0,0,0;3,0,0,0]*	3/2	0	0	0	1/2	0	0	0	0	0
[0,0,0,0,0,0;3,2,1,0]*	5	0	0	0	0	0	0	0	0	0
[0,0,0,0,0,0;3,1,2,0]*	5	0	0	0	0	0	0	0	0	0
[1,0,0,0,0,0;3,2,0,0]*	5	0	0	0	0	0	0	0	0	0
[1,0,0,0,0,0;3,0,2,0]*	5	0	0	0	0	0	0	0	0	0
[2,0,0,0,0,0;3,1,0,0]*	5	0	0	0	0	0	0	0	0	0
[2,0,0,0,0,0;3,0,1,0]*	5	0	0	0	0	0	0	0	0	0
[2,1,0,0,0,0;3,0,0,0]*	5	0	0	0	0	0	0	0	0	0
[0,0,0,0,0,0;3,1,1,1]*	10	0	0	0	0	0	0	0	0	0
[1,0,0,0,0,0;3,1,1,0]*	10	0	0	0	0	0	0	0	0	0
[1,0,0,0,0,0;3,0,1,1]*	10	0	0	0	0	0	0	0	0	0
[1,1,0,0,0,0;3,1,0,0]*	10	0	0	0	0	0	0	0	0	0
[1,1,0,0,0,0;3,0,1,0]*	10	0	0	0	0	0	0	0	0	0
[1,1,1,0,0,0;3,0,0,0]*	10	0	0	0	0	0	0	0	0	0
[0,0,0,0,0,0;2,2,2,0]*	6	3	0	0	0	0	0	0	0	0
[2,0,0,0,0,0;2,2,0,0]	5	2	1	1	0	2	0	0	0	0
[2,0,0,0,0,0;2,0,2,0]*	6	3	0	0	0	0	0	0	0	0
[2,2,0,0,0,0;2,0,0,0]*	6	3	0	0	0	0	0	0	0	0
[0,0,0,0,0,0;2,2,1,1]	13	0	0	4	0	0	0	0	0	0
[0,0,0,0,0,0;2,1,2,1]*	15	0	0	0	0	0	0	0	0	0
[1,0,0,0,0,0;2,2,1,0]*	15	0	0	0	0	0	0	0	0	0
[1,0,0,0,0,0;2,2,0,1]*	15	0	0	0	0	0	0	0	0	0
[1,1,0,0,0,0;2,2,0,0]	13	0	4	0	0	0	0	0	0	0
[1,1,0,0,0,0;2,0,2,0]*	15	0	0	0	0	0	0	0	0	0
[2,0,0,0,0,0;2,1,1,0]*	15	0	0	0	0	0	0	0	0	0
[2,1,0,0,0,0;2,1,0,0]*	15	0	0	0	0	0	0	0	0	0
[2,1,0,0,0,0;2,0,1,0]*	15	0	0	0	0	0	0	0	0	0
[2,1,1,0,0,0;2,0,0,0]*	15	0	0	0	0	0	0	0	0	0
[1,0,0,0,0,0;2,1,1,1]*	30	0	0	0	0	0	0	0	0	0
[1,1,0,0,0,0;2,1,1,0]*	30	0	0	0	0	0	0	0	0	0
[1,1,0,0,0,0;2,0,1,1]*	30	0	0	0	0	0	0	0	0	0

Table 1 continued

	$\mathbf{C}_1$	$\mathbf{C}_2$	$\mathbf{C}_s$	$\mathbf{C}'_s$	$\mathbf{C}_3$	$\mathbf{C}_{2v}$	$\mathbf{C}_{3v}$	$\mathbf{C}_{3h}$	$\mathbf{D}_3$	$\mathbf{D}_{3h}$
[1,1,1,0,0,0;2,1,0,0]*	30	0	0	0	0	0	0	0	0	0
[1,1,1,0,0,0;2,0,1,0]*	30	0	0	0	0	0	0	0	0	0
[1,1,1,1,0,0;2,0,0,0]*	30	0	0	0	0	0	0	0	0	0
[1,1,1,1,0,0;1,1,0,0]	60	0	0	0	0	0	0	0	0	0

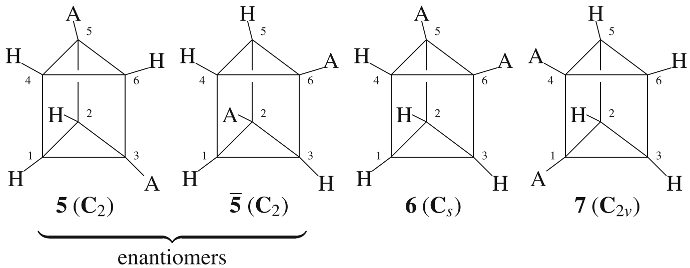

Fig. 3 Prismane derivatives of the constitution H_4A_2 (partition $[\theta]_1 = [4, 2, 0, 0, 0, 0; 0, 0, 0, 0]$). The letter *A* represents an achiral proligand in isolation

The $\mathbf{C}_{2v}$-promolecule **7** provides us with an extended prochirality in a geometric meaning. The $\mathbf{C}_{2v}$-promolecule **7** is fixed (stabilized) under the action of the $\mathbf{C}_{2v}$-group:

$$\begin{aligned}\mathbf{C}_{2v} &= \{I, C_{2(1)}, \sigma_h, \sigma_{v(1)}\} \\ &\sim \{(1)(2)(3)(4)(5)(6), (1\ 4)(2\ 6)(3\ 5), \\ &\quad \overline{(1\ 4)(2\ 5)(3\ 6)}, \overline{(1)(2\ 3)(4)(5\ 6)}\},\end{aligned} \tag{40}$$

which exhibits a separation into two orbits, $\{1, 4\}$ and $\{2, 3, 5, 6\}$. According to Table 12 of Ref. [25] (Appendix C.13 of [26] contains a misprint) from a viewpoint of subduction, the $\mathbf{C}_{2v}$-promolecule **7** is generated in terms of the following subduction:

$$\mathbf{D}_{3h}(/\mathbf{C}_s) \downarrow \mathbf{C}_{2v} = \underbrace{\mathbf{C}_{2v}(/\mathbf{C}_1)}_{\{2,3,5,6\}} + \underbrace{\mathbf{C}_{2v}(/\mathbf{C}_s)}_{\{1,4\}}, \tag{41}$$

which correspond to the USCI-CF a_2c_4 (Eq. 9). Two achiral proligands A's occupy the two-membered homospheric $\mathbf{C}_{2v}(/\mathbf{C}_s)$-orbits, i.e., $\{1, 4\}$, while four hydrogens (as achiral proligands) occupy the four-membered enantiospheric $\mathbf{C}_{2v}(/\mathbf{C}_1)$-orbit, i.e., $\{2, 3, 5, 6\}$. The presence of one enantiospheric orbit indicates that the $\mathbf{C}_{2v}$-promolecule **7** is prochiral in a geometric meaning.

Prochirality due to the presence of enantiospheric orbit(s) is a clue for testifying the possibility of chiral (asymmetric) syntheses. For example, a potential chiral synthesis generating a $\mathbf{C}_2$-promolecule (**9** or $\overline{\mathbf{9}}$) from a $\mathbf{C}_{2v}$-promolecule (**8**) is shown

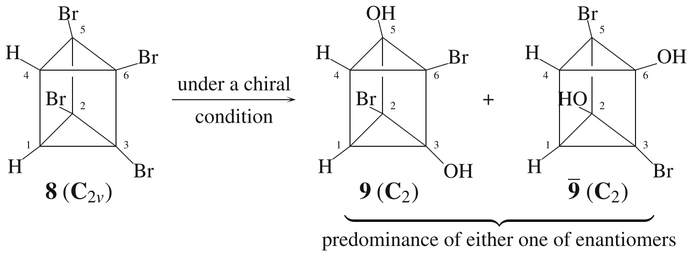

Fig. 4 Participation of an enantiospheric orbit of four bromine atoms in a potential chiral synthesis

in Fig. 4, where four bromine atoms in the four-membered enantiospheric $\mathbf{C}_{2v}(/\mathbf{C}_1)$-orbit are divided into two halves under a chiral condition (such as the attack of a chiral reagent). The starting $\mathbf{C}_{2v}$-promolecule (**8**) is generated by the subduction of Eq. (41) in a parallel way to the $\mathbf{C}_{2v}$-promolecule **7**. Note that the constitution H_2Br_4 (or the term H^2Br^4) also corresponds to the partition $[\theta]_1$ (= [4, 2, 0, 0, 0, 0; 0, 0, 0, 0]). The product $\mathbf{C}_2$-promolecules (**9**/$\overline{\mathbf{9}}$) are generated by the same subduction as the $\mathbf{C}_2$-promolecules (**5**/$\overline{\mathbf{5}}$). This type of potential chiral syntheses has been discussed by using ethylene oxides as examples in Ref. [20] and in Chapter 10 of Ref. [26].

Geometrically speaking, the potential chiral synthesis shown in Fig. 4 is regarded as a further restriction of the $\mathbf{C}_{2v}$-symmetry to the $\mathbf{C}_2$-symmetry, which is characterized by the subduction of the coset representation $\mathbf{C}_{2v}(/\mathbf{C}_1)$ as follows:

$$\mathbf{C}_{2v}(/\mathbf{C}_1) \downarrow \mathbf{C}_2 = \underbrace{2\mathbf{C}_2(/\mathbf{C}_1)}_{\{2,6\},\,\{3,5\}}, \tag{42}$$

which is collected in Table C.5 of Appendix C of Ref. [26]. Thereby, the $\mathbf{C}_{2v}(/\mathbf{C}_1)$-orbit of the four bromine atoms in **8**, i.e., {2, 3, 5, 6}, is subdivided into two $\mathbf{C}_2(/\mathbf{C}_1)$-orbits, i.e., {2, 6} and {3, 5}, either of which is attacked by hydrolysis reagents under a chiral condition.

In the conventional terminology, prochirality has been detected a combination of the terms *enantiotopic* (relationship) and *chirotopic* (local symmetry) proposed by Mislow and Siegel [12], where the original term *enantiotopic* is concerned mainly with a relationship between two objects and the original term *chirotopic* is concerned with the local symmetry as an attribute of a single site. The necessity of this combination of a relational term with an attributive term stems from the fact that the conventional terminology has lacks the concepts of orbits and sphericities.

In contrast, prochirality due to the presence of enantiospheric orbit(s) is based on the concepts of orbits and their sphericities, where the terms *sphericities* are concerned with the attributes of orbits governed by coset representations. This feature is effective to discuss such complicated cases as shown in Fig. 4. Note that the derivation of **7** or **8** from a prismane skeleton **1** is characterized by the subduction of Eq. (41), while the derivation of chiral products **9**/$\overline{\mathbf{9}}$ from an achiral prismane derivative **8** is characterized by the subduction of Eq. (42). Thus, these two types of processes for derivation can be discussed commonly by the subduction and sphericities of orbits.

Fig. 5 Prismane derivatives of the constitution $H_4p\overline{p}$ (partition $[\theta]_5 = [4, 0, 0, 0, 0, 0; 1, 1, 0, 0]$). A pair of p and $\bar{p}$ represents a pair of enantiomeric proligands in isolation

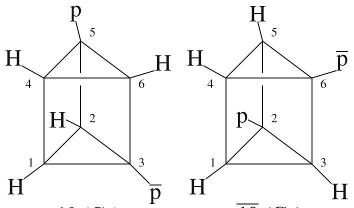

10 ($\mathbf{C}_1$) $\overline{\mathbf{10}}$ ($\mathbf{C}_1$)

enantiomers

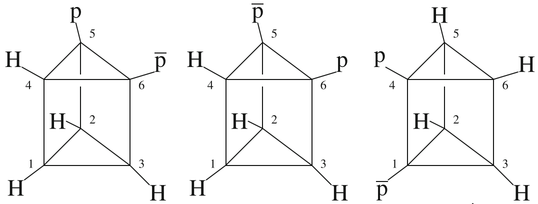

11 ($\mathbf{C}_s$) **12** ($\mathbf{C}_s$) **13** ($\mathbf{C}'_s$)

5.2 Extended pseudoasymmetry

The FPM method (the $[\theta]_5$-row of Eq. 28) and the PCI method (the [4, 0, 0, 0, 0, 0; 1, 1, 0, 0]-row of Table 1) indicates the presence of one pair of enantiomeric $\mathbf{C}_1$-promolecules, two $\mathbf{C}_s$-promolecules, and one $\mathbf{C}'_s$-promolecule for prismanes with the constitution $H_4p\overline{p}$. They are depicted in Fig. 5.

The two $\mathbf{C}_s$-promolecules **11** and **12** are generated in terms of the subduction of Eq. (5) or of the corresponding USCI-CF $a_1^2c_2^2$ (Eq. 9). A pair of p/$\overline{p}$ as enantiomeric proligands in isolation occupy the two-membered enantiospheric $\mathbf{C}_s(/\mathbf{C}_1)$-orbit, i.e., {5, 6}, two hydrogens (as achiral proligands) occupy the other two-membered enantiospheric $\mathbf{C}_s(/\mathbf{C}_1)$-orbit, i.e., {2, 3}, and the remaining hydrogens separately occupy two one-membered homospheric $\mathbf{C}_s(/\mathbf{C}_s)$-orbits, i.e., {1} and {4}, one by one. The presence of two enantiospheric orbits indicates that the $\mathbf{C}_s$-promolecule **11** or **12** is prochiral in a geometric meaning. The two proligands (p and $\overline{p}$) or the two hydrogens of the enantiospheric orbit are differentiated under a chiral condition so as to generate promolecules of enantiomeric relationships.

Each of the two $\mathbf{C}_s$-promolecules **11** and **12** is fixed (stabilized) under the action of the following $\mathbf{C}_s$-group:

$$\mathbf{C}_s = \{I, \sigma_{v(1)}\} \sim \{(1)(2)(3)(4)(5)(6), \overline{(1)(2\ 3)(4)(5\ 6)}\}, \tag{43}$$

which is a subgroup of $\mathbf{D}_{3h}$ shown in Eqs. (3) and (4). These $\mathbf{C}_s$-promolecules are interchangeable to each other under the action of the following $\widetilde{\mathbf{C}}_s$-group:

$$\widetilde{\mathbf{C}}_s = \{I, \widetilde{\sigma}_{v(1)}\} \sim \{(1)(2)(3)(4)(5)(6), (1)(2\ 3)(4)(5\ 6)\}, \tag{44}$$

which is accompanied by no alteration of ligand chirality senses. In other words, the two $\mathbf{C}_s$-promolecules **11** and **12** exhibit pseudoasymmetry in an extended meaning. It should be noted that a more extended group (i.e., an *RS*-stereoisomeric group on the basis of the stereoisogram approach) is necessary to comprehend this type of pseudoasymmetry, as discussed in an accompanying paper of this series.

On the other hand, the $\mathbf{C}'_s$-promolecule **13** is generated in terms of the following subduction:

$$\mathbf{D}_{3h}(/\mathbf{C}_s) \downarrow \mathbf{C}'_s = \underbrace{3\mathbf{C}'_s(/\mathbf{C}_1)}_{\{1,4\},\ \{2,5\},\ \{3,6\}} \tag{45}$$

which correspond to USCI-CF c_2^3 (Eq. 9). A pair of p/$\overline{\text{p}}$ as enantiomeric proligands in isolation occupy the two-membered enantiospheric $\mathbf{C}'_s(/\mathbf{C}_1)$-orbit, i.e., $\{1, 4\}$, while two pairs of hydrogens (as achiral proligands) occupy the other two-membered enantiospheric $\mathbf{C}'_s(/\mathbf{C}_1)$-orbits, i.e., $\{2, 5\}$, and $\{3, 6\}$. The presence of three enantiospheric orbits indicates that the $\mathbf{C}'_s$-promolecule **13** is prochiral in a geometric meaning. The two proligands (p and $\overline{\text{p}}$) or the two hydrogens of each enantiospheric orbit are differentiated under a chiral condition so as to generate promolecules of enantiomeric relationships.

The $\mathbf{C}'_s$-promolecule **13** is fixed (stabilized) under the action of the following $\mathbf{C}'_s$-group:

$$\mathbf{C}'_s = \{I, \sigma_h\} \sim \{(1)(2)(3)(4)(5)(6), \overline{(1\ 4)(2\ 5)(3\ 6)}\}, \tag{46}$$

which is a subgroup of $\mathbf{D}_{3h}$ shown in Eqs. (3) and (4). The $\mathbf{C}_s$-promolecule **13** is converted into a homomer, which is identical with the original **13** under the action of the following $\widetilde{\mathbf{C}}'_s$-group:

$$\widetilde{\mathbf{C}}'_s = \{I, \widetilde{\sigma}_h\} \sim \{(1)(2)(3)(4)(5)(6), (1\ 4)(2\ 5)(3\ 6)\}, \tag{47}$$

which is accompanied by no alteration of ligand chirality senses. In other words, the $\mathbf{C}_s$-promolecule **13** exhibit a meso-type behavior in an extended meaning. It should be noted that a more extended group (i.e., an *RS*-stereoisomeric group on the basis of the stereoisogram approach) is necessary to comprehend this meso-type behavior, as discussed in an accompanying paper of this series.

As promolecules having the constitution H_4p_2 or $\text{H}_4\overline{\text{p}}_2$ ($[\theta]_2 = [4, 0, 0, 0, 0, 0; 2, 0, 0, 0]$), Fig. 6 shows one pair of $\mathbf{C}_1$-promolecules (**14**/$\overline{\mathbf{14}}$) and three pairs of $\mathbf{C}_2$-promolecules (**15**/$\overline{\mathbf{15}}$, **16**/$\overline{\mathbf{16}}$, and **17**/$\overline{\mathbf{17}}$) in accord with the enumeration results by the FPM method (the $[\theta]_2$-row of Eq. 28) and by the PCI method (the $[4, 0, 0, 0, 0, 0; 2, 0, 0, 0]$-row of Table 1). Note that each number of promolecules appears as a multiple of the term $\frac{1}{2}(\text{H}^4\text{p}^2 + \text{H}^4\overline{\text{p}}^2)$, because a pair of enantiomers is counted once.

The $\mathbf{C}_1$-promolecule **14** is converted into $\overline{\mathbf{14}}$ under the action of $\mathbf{C}_s$ (Eq. 43), while **14** is fixed (stabilized) under the action of $\widetilde{\mathbf{C}}_s$ (Eq. 44). This behavior is an extension of the "prochirality" proposed by Hanson [11], where **14** is already chiral in spite of its "prochirality". This behavior should be characterized by pro-*RS*-stereogenicity on

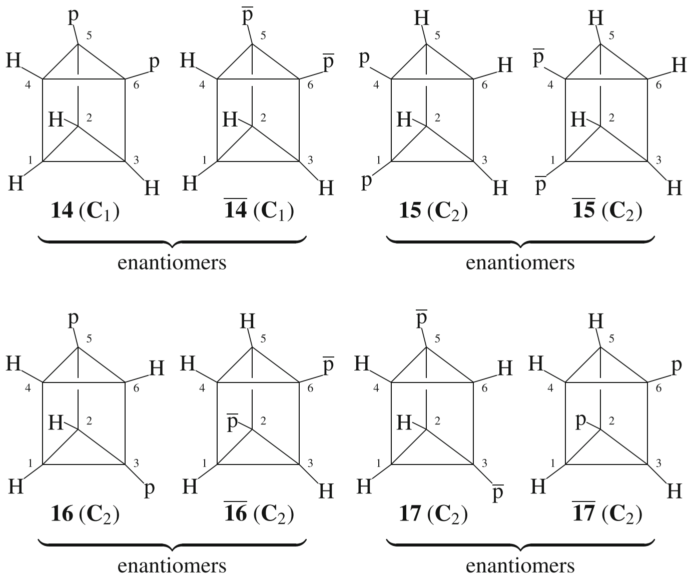

Fig. 6 Prismane derivatives of the constitution H_4p^2 or $H_4\bar{p}^2$ (partition $[\theta]_2 = [4, 0, 0, 0, 0, 0; 2, 0, 0, 0]$). A pair of p and $\bar{p}$ represents a pair of enantiomeric proligands in isolation

the basis of the stereoisogram approach, as discussed in an accompanying paper of this series.

The $\mathbf{C}_2$-promolecule **15** is converted into its enantiomer $\overline{\mathbf{15}}$ under the action of the $\mathbf{C}_{2v}$-group (Eq. 40). When we take account of permutations with no ligand reflection, we obtain the following group:

$$\begin{aligned}\widetilde{\mathbf{C}}_{2v} &= \{I, C_{2(1)}, \widetilde{\sigma}_h, \widetilde{\sigma}_{v(1)}\} \\ &\sim \{(1)(2)(3)(4)(5)(6), (1\ 4)(2\ 6)(3\ 5), \\ &\quad (1\ 4)(2\ 5)(3\ 6), (1)(2\ 3)(4)(5\ 6)\},\end{aligned} \tag{48}$$

The $\mathbf{C}_2$-promolecule **15** (or $\overline{\mathbf{15}}$) is fixed (stabilized) under the action of $\widetilde{\mathbf{C}}_{2v}$ (Eq. 48). This behavior is an extension of the "prochirality" proposed by Hanson [11], where **15** is already chiral in spite of its "prochirality". A parallel discussion holds true for a pair of $\mathbf{C}_2$-promolecules **16**/$\overline{\mathbf{16}}$ or a pair of $\mathbf{C}_2$-promolecules **17**/$\overline{\mathbf{17}}$. The behaviors of these pairs should be characterized by pro-*RS*-stereogenicity on the basis of the stereoisogram approach, as discussed in an accompanying paper of this series.

5.3 Geometric prochirality and extended pseudoasymmetry

Extended pseudoasymmetry is accompanied by geometric prochirality (prochirality in a purely geometric meaning) because of the presence of one or more enantiospheric orbits. For example, a $\mathbf{C}_{2v}$-promolecule **18** (or **20**) is fixed (stabilized) under the $\mathbf{C}_{2v}$-group (Eq. 40). Note that the [2, 0, 0, 0, 0, 0; 2, 2, 0, 0]-row of Table 1 shows the

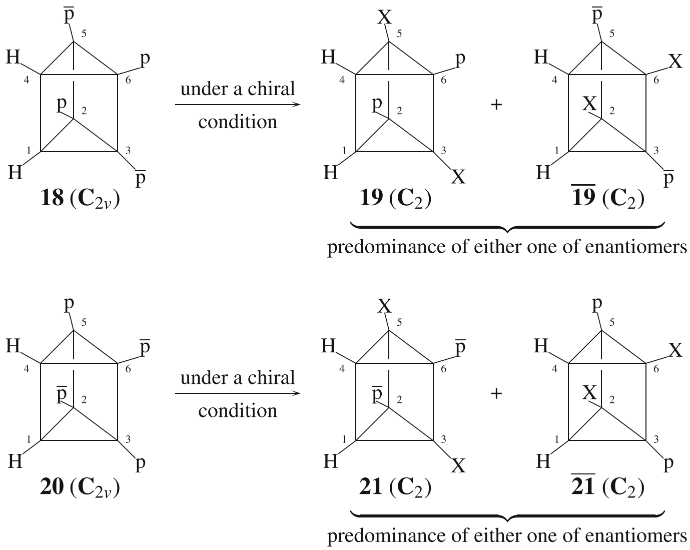

Fig. 7 Participation of an enantiospheric orbit of $p^2\overline{p}^2$ in a potential chiral synthesis

presence of two $\mathbf{C}_{2v}$-promolecules. The six substitution sites of **18** (or **20**) are divided into two orbits according to the subduction represented by Eq. (41). The resulting four-membered $\mathbf{C}_{2v}(/\mathbf{C}_1)$-orbit {2, 3, 5, 6} accommodates two p's and two $\overline{\text{p}}$'s according to its enantiosphericity. Because of the enantiosphericity, the $\mathbf{C}_{2v}$-promolecule **18** (or **20**) is prochiral so as to be capable of undergoing chiral syntheses shown in Fig. 7.

The potential chiral syntheses shown in Fig. 7 are characterized by the subduction represented by Eq. (42). Thereby, the $\mathbf{C}_{2v}(/\mathbf{C}_1)$-orbit of $p^2\overline{p}^2$ in **18** (or **20**) is subdivided into two $\mathbf{C}_2(/\mathbf{C}_1)$-orbits, i.e., {2, 6} and {3, 5}, either of which is attacked by appropriate reagents (X) under a chiral condition, as shown in Fig. 7.

Extended pseudoasymmetry between **18** and **20** is ascribed to their interconvertibility under the action of the $\widetilde{\mathbf{C}}_{2v}$-group (Eq. 48). It should be noted again that a more extended group (i.e., an *RS*-stereoisomeric group on the basis of the stereoisogram approach) is necessary to comprehend this type of pseudoasymmetry, as discussed in an accompanying paper of this series.

6 Conclusions

The FPM method and PCI method of the USCI approach have been applied to the combinatorial enumeration of prismane derivatives on the basis of the proligand-promolecule model, which enables us to take account of achiral and chiral proligands. Prochirality in a geometric meaning has been discussed in general by emphasizing the presence of enantiospheric orbits in enumerated prismane derivatives. In particular, chiral proligands along with achiral ones are clarified to participate in the appearance of prochirality. On the other hand, the scope of pseudoasymmetry has been extended to cover such a rigid skeleton as prismane in place of a usual pseudoasymmetric center as a single atom, where the proligand-promolecule model works well as a key.

References

1. J.H. van't Hoff, *La Chimie Dans L'Espace* (P. M. Bazendijk, Rotterdam, 1875)
2. J.H. van't Hoff, *Die Lagerung der Atome im Raume, (German Translation by F. Herrmann)* (Friedrich Vieweg und Sohn, Braunschweig, 1877)
3. J.A. Le Bel, Bull. Soc. Chim. Fr. (2) **22**, 337–347 (1874)
4. E. Fischer, *Aus meinem Leben* (Springer, Berlin, 1922)
5. E. Fischer, Ber. Dtsch. Chem. Ges. **24**, 1836–1845 (1891)
6. E. Fischer, Ber. Dtsch. Chem. Ges. **24**, 2683–2687 (1891)
7. R.S. Cahn, C.K. Ingold, V. Prelog, Angew. Chem. Int. Ed. Eng. **5**, 385–415 (1966)
8. V. Prelog, G. Helmchen, Angew. Chem. Int. Ed. Eng. **21**, 567–583 (1982)
9. V. Prelog, G. Helmchen, Helv. Chim. Acta **55**, 2581–2598 (1972)
10. V. Prelog, Science **193**, 17–24 (1976)
11. K.R. Hanson, J. Am. Chem. Soc. **88**, 2731–2742 (1966)
12. K. Mislow, J. Siegel, J. Am. Chem. Soc. **106**, 3319–3328 (1984)
13. IUPAC Organic Chemistry Division, Pure Appl. Chem. **68**, 2193–2222 (1996)
14. G. Pólya, Acta Math. **68**, 145–254 (1937)
15. G. Pólya, R.C. Read, *Combinatorial Enumeration of Groups, Graphs, and Chemical Compounds* (Springer, New York, NY, 1987)
16. S. Fujita, Croat. Chem. Acta **79**, 411–427 (2006)
17. R.W. Robinson, F. Harary, A.T. Balaban, Tetrahedron **32**, 355–361 (1976)
18. S. Fujita, Theor. Chim. Acta **76**, 247–268 (1989)
19. S. Fujita, J. Math. Chem. **5**, 99–120 (1990)
20. S. Fujita, J. Am. Chem. Soc. **112**, 3390–3397 (1990)
21. S. Fujita, Bull. Chem. Soc. Jpn. **74**, 1585–1603 (2001)
22. S. Fujita, Chem. Rec. **2**, 164–176 (2002)
23. S. Fujita, Bull. Chem. Soc. Jpn. **75**, 1863–1883 (2002)
24. S. Fujita, Bull. Chem. Soc. Jpn. **63**, 203–215 (1990)
25. S. Fujita, Bull. Chem. Soc. Jpn. **63**, 315–327 (1990)
26. S. Fujita, *Symmetry and Combinatorial Enumeration in Chemistry* (Springer, Berlin, Heidelberg, 1991)
27. S. Fujita, Tetrahedron **47**, 31–46 (1991)
28. S. Fujita, J. Chem. Inf. Comput. Sci. **32**, 354–363 (1992)
29. S. Fujita, Polyhedron **12**, 95–110 (1993)
30. S. Fujita, J. Chem. Educ. **63**, 744–746 (1986)
31. S. Fujita, J. Chem. Inf. Comput. Sci. **40**, 426–437 (2000)
32. S. Fujita, Bull. Chem. Soc. Jpn. **73**, 2679–2685 (2000)
33. S. Fujita, J. Chem. Inf. Comput. Sci. **31**, 540–546 (1991)
34. S. Fujita, Bull. Chem. Soc. Jpn. **75**, 1949–1962 (2002)
35. S. Fujita, Bull. Chem. Soc. Jpn. **63**, 1876–1883 (1990)
36. S. Fujita, J. Chem. Inf. Comput. Sci. **39**, 151–163 (1999)
37. S. Fujita, MATCH Commun. Math. Comput. Chem. **46**, 25–44 (2002)
38. S. Fujita, Helv. Chim. Acta **85**, 2440–2457 (2002)
39. S. Fujita, Bull. Chem. Soc. Jpn. **63**, 2759–2769 (1990)
40. S. Fujita, Tetrahedron **46**, 5943–5954 (1990)
41. S. Fujita, Bull. Chem. Soc. Jpn. **64**, 439–449 (1991)
42. S. Fujita, Bull. Chem. Soc. Jpn. **64**, 3215–3223 (1991)
43. S. Fujita, Bull. Chem. Soc. Jpn. **84**, 1192–1207 (2011)
44. S. Fujita, Theor. Chem. Acc. **113**, 73–79 (2005)
45. S. Fujita, Theor. Chem. Acc. **113**, 80–86 (2005)
46. S. Fujita, Theor. Chem. Acc. **115**, 37–53 (2006)
47. S. Fujita, Theor. Chem. Acc. **117**, 353–370 (2007)
48. S. Fujita, Theor. Chem. Acc. **117**, 339–351 (2007)
49. S. Fujita, MATCH Commun. Math. Comput. Chem. **67**, 5–24 (2012)

50. S. Fujita, MATCH Commun. Math. Comput. Chem. **67**, 25–54 (2012)
51. S. Fujita, *Diagrammatical Approach to Molecular Symmetry and Enumeration of Stereoisomers* (University of Kragujevac, Faculty of Science, Kragujevac, 2007)
52. S. Fujita, MATCH Commun. Math. Comput. Chem. **57**, 5–48 (2007)
53. S. Fujita, J. Org. Chem. **67**, 6055–6063 (2002)